Available online at www.sciencedirect.com
ScienceDirect
Trans. Nonferrous Met. Soc. China 25(2015) 2533−2542
Transactions of Nonferrous Metals Society of China
www.tnmsc.cn

Microstructures and mechanical properties of metal inert-gas arc welded Mg−steel dissimilar joints

Xiao-yong WANG, Da-qian SUN, Shi-qiang YIN, Dong-yang LIU

Key Laboratory of Automobile Materials of Ministry of Education,
School of Materials Science and Engineering, Jilin University, Changchun 130025, China

Received 20 October 2014; accepted 25 January 2015

Abstract: The joining of Mg alloy to steel was realized by metal inert-gas arc welding, and the weld thermal cycle characteristics and Mg−steel joints were investigated. The results show that the temperature distribution in the joints is uneven. Mg alloy welds present a fine equiaxed grain structure. There exists a transition layer consisting mainly of AlFe, $AlFe_3$ and $Mg(Fe, Al)_2O_4$ phases at Mg/steel interface, and it is the weakest link in Mg−steel joints. The welding heat input and weld Al content have the significant effect on the joint strength. The joint strength increases with increasing the heat input from 1680 J/cm to 2093 J/cm, due to promoting Mg/steel interface reaction. When weld Al content is increased to 6.20%, the joint strength reaches 192 MPa, 80% of Mg alloy base metal strength. It is favorable to select the suitable welding heat input and weld Al content for improving joint strength.

Key words: AZ31B Mg alloy; Q235 steel; metal inert-gas arc welding; dissimilar metal joining

1 Introduction

Magnesium and its alloys have been suggested in transport applications to reduce the fuel consumption and environmental pollution, due to their unique characteristics such as low density, high specific strength along with good damping capacity [1−5]. It is well known that steels are the most common metal materials in transport industry [6]. Hybrid structures of Mg alloy to steel have a widely applied prospect in the field of automotive and railway vehicle industries [7]. Therefore, it has received remarkable attention to joining Mg alloy and steel dissimilar metals.

Some difficulties are encountered in dissimilar welding of Mg alloy and steel. The difficulties mainly result from the great difference between their melting points (649 °C for Mg and 1535 °C for Fe) and the nearly zero solubility of Mg and Fe [8]. In addition, Mg and Fe do not react with each other to form binary compounds at ambient pressure [9]. There are some research activities on joining Mg alloy to steel in recent years. The current methods are generally limited to the solid-state welding processes, such as the diffusion welding [10,11], the friction stir welding [8,12] and the resistance spot welding [13,14]. However, their application is limited by the geometry and size of workpiece, and the mechanical properties of welded joints achieved by these processes are also not satisfactory. The hybrid laser-TIG welding [15−18] and laser penetration brazing (LPB) [19,20] were also used for joining Mg alloy to steel. The results showed that the Ni interlayer favors improving the microstructure and tensile shear strength of Mg−steel joints produced by the hybrid laser-TIG welding. For the LPB, the transition layer at Mg/steel interface region consisted mainly of intermetallic compounds and metal oxides, and the joint strength reached a maximum of 185 MPa at 0.6 mm laser offset.

Metal inert-gas arc welding (MIG welding) is widely applied in automobile and railway vehicle industries for its high efficiency, low cost and good applicability for the geometry and size of workpiece [21,22]. Therefore, it is of important significance to realize the MIG welding of Mg alloy to steel for mass serial production. However, up to now, the report dealing with the MIG welding of Mg alloy and steel is very limited. The present work investigates microstructures and mechanical properties of MIG welded Mg−steel joints produced with different welding heat inputs and

Corresponding author: Shi-qiang YIN; Tel/Fax: +86-431-85094687; E-mail: ysq@jlu.edu.cn
DOI: 10.1016/S1003-6326(15)63872-9

filler metals. The purpose is to better understand the weldability of Mg alloy and steel, and to provide some foundation for improving mechanical properties of the Mg−steel joints.

2 Experimental

In this investigation, AZ31B Mg alloy and Q235 low carbon steel plates with dimensions of 200 mm× 50 mm×3mm were employed as base metals, and Mg alloy welding wires (AZ31 and AZ61) with a diameter of 1.6 mm were chosen as filler metals. Chemical compositions and mechanical properties of them are listed in Table 1, Table 2 and Table 3, respectively. The Mg alloy base metal has an equiaxed grain structure consisting of α(Mg) solid solution, and the grain size is about 20 μm. The phase composition of the low carbon steel is mainly α(Fe) phase.

Table 1 Chemical compositions of Mg alloy and low carbon steel base metals (mass fraction, %)

Base metal	Al	Zn	Mn	Si
AZ31B alloy	3.4	0.7	0.2	0.043
Q235 steel	–	–	0.45	0.20
Base metal	C	S	P	Fe	Mg
AZ31B alloy	–	–	–	0.003	Bal.
Q235 steel	0.17	0.021	0.015	Bal.	–

Table 2 Chemical compositions of Mg alloy filler metals (mass fraction, %)

Filler metal	Al	Zn	Mn	Si
AZ31	3.13	0.73	0.35	0.005
AZ61	6.63	0.71	0.25	0.015
Filler metal	Fe	Cu	Ni	Mg
AZ31	0.003	0.005	0.001	Bal.
AZ61	0.003	0.005	0.001	Bal.

Table 3 Mechanical properties of Mg alloy and low carbon steel base metals

Base metal	Tensile strength/MPa	Yield strength/MPa	Elongation/ %
AZ31B alloy	240	130	18
Q235 steel	375	235	21

Prior to welding, the single groove was machined in the Mg alloy and low carbon steel plates, the bevel angles of Mg and steel plates were 30° and 45° respectively, and then both plates were assembled into a single V-groove with a root opening of 1 mm. The welding of Mg alloy and steel was made using the metal inert-gas arc welding (MIG welding) with Ar shielding gas. During MIG welding, the Mg alloy filler metal wire was directed toward the middle of the steel groove face by welding torch, and was deposited in the V-groove at different welding heat inputs, as shown in Fig. 1. The torch has a drag angle along the welding direction for improving the liquid Mg spreading on solid steel surface and the Mg weld appearance. The welding heat input (E) represents the amount of heat input per unit length of weld, and is determined according

$$E = \eta IU/v \tag{1}$$

where I is the welding current, U is the arc voltage, v is the welding speed, and η is the heat source efficiency, a constant of 0.7 for the MIG welding process.

The weld thermal cycles in Mg alloy weld and Mg/steel interface were measured using embedded thermocouples. Four holes with 1 mm in diameter were machined in test plates for the placement of thermocouples (TC1, TC2, TC3 and TC4), and high temperature epoxy was used to fix the thermocouples. The layout of the locations of the thermocouples is shown in Fig. 2. During MIG welding, a digital data logger with a total capacity of eight K-type thermocouples was used to record the weld thermal cycles, the thermocouples TC1, TC2, and TC3 for the top, middle and bottom of Mg/steel interfaces, respectively, and TC4 for weld adjacent to the Mg alloy base metal.

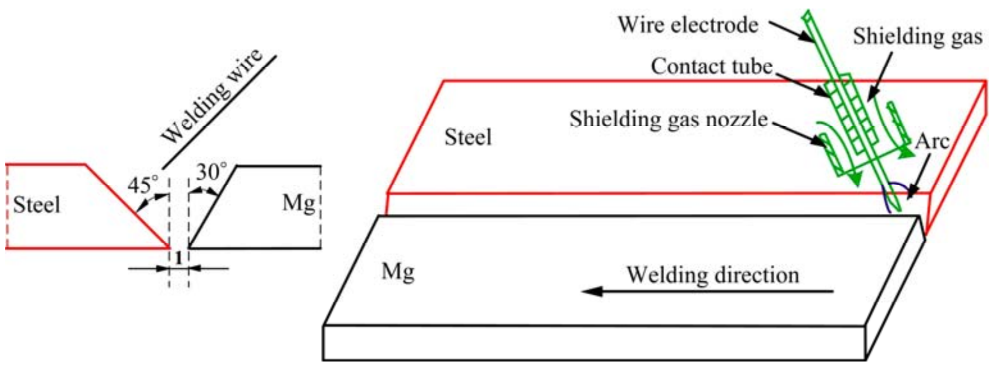

Fig.1 Schematic diagram of MIG welding

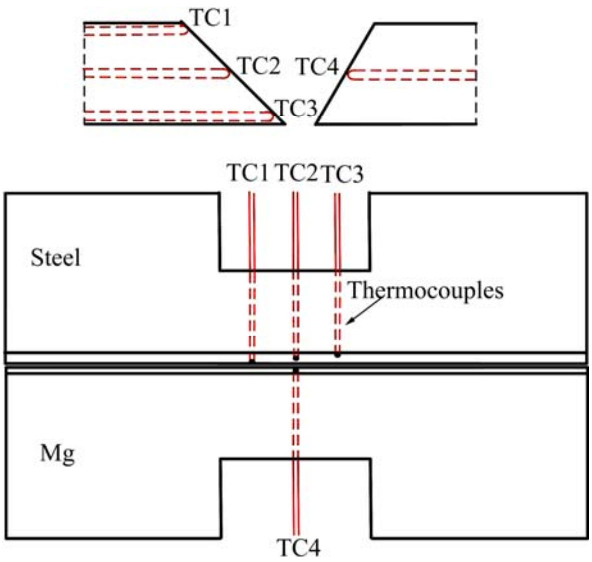

Fig. 2 Layout of locations of thermocouples

After the welding, Mg−steel joint specimens were cut down from the welded plates. The joint specimens were ground, polished and then etched in the picric acid etchant solution. The nital was also used for steel HAZ. The microstructure and composition of Mg−steel joints were examined by using optical microscope (OM, PMG3), scanning electron microscope (SEM, EVO18) equipped with energy dispersive X-ray spectroscope (EDS, Link-ISIS), transmission electron microscope (TEM, JEM−2100F) and X-ray diffraction (XRD, D/Max 2500PC). The Vickers microhardness of the joints was measured with a load of 50 g and a duration time of 10 s. The tensile test of Mg−steel joints was carried out using the MT810 universal material testing system at room temperature.

3 Results and discussion

3.1 Weld thermal cycle characteristics

The weld thermal cycle represents the temperature distribution and gradient in welded joints during welding. It would be extremely useful to reveal weld thermal cycle characteristics for understanding the changes of microstructures and properties of the joints. Since the temperature distribution at Mg/steel interface is of particular interest for joining Mg to steel, weld thermal cycles at the interface and weld were measured using embedded thermocouples (Fig. 2). Thermocouples TC1, TC2 and TC3 were used to measure the weld thermal cycles at the top, middle and bottom of Mg/steel interfaces, respectively, while TC4 stood for that of weld.

Figure 3 shows the weld thermal cycle curves recorded by thermocouples during MIG welding at the

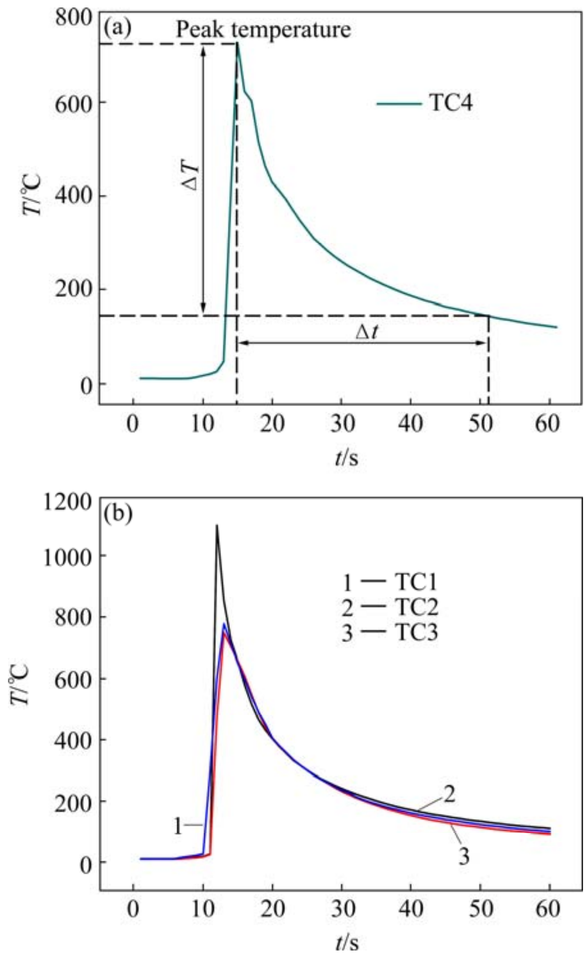

Fig. 3 Weld thermal cycle curves: (a) Weld; (b) Mg/steel interface

welding current of 135 A, arc voltage of 24 V and welding speed of 65 cm/min. The peak temperatures, heating and cooling rates of the weld thermal cycles are given in Table 4. From Fig. 3(a), it can be seen that the weld has very quick heating and cooling rates (89.2 °C/s and 16.0 °C/s), at the peak temperature of 725.4 °C, which will increase the nucleation rate and form the fine grain weld metal. During the weld cooling, the cooling rate becomes relatively slow in the temperature range of 625−585 °C, indicating the phase transformation occurring from liquid Mg to solid α(Mg) in this temperature range.

Figure 3(b) shows the weld thermal cycle curves for the top (TC1), middle (TC2) and bottom (TC3) of Mg/steel interface. The heating and cooling rates of the interface are also very quick, and there is a significant difference in peak temperatures. The middle of the Mg/steel interface has the highest peak temperature (1097.7 °C), and the lowest peak temperature (747.8 °C) appears in the interface bottom. It can be explained by the power density distribution of MIG arc heat source. In this investigation, the magnesium alloy filler metal electrode was directed toward the middle of steel groove face, and the arc was established between the anode spot at tip of the filler metal and the cathode spot in the middle of the steel groove face. Since the power density distribution of the heat source was considered Gaussian [23], hence the middle of Mg/steel interface has the highest power density and peak temperature. These characteristics of weld thermal cycles should affect microstructures and mechanical properties of MIG welded Mg−steel joints.

Table 4 Peak temperature, heating rate and cooling rate of weld thermal cycle

Thermocouple	Peak temperature/°C	Heating rate/(°C·s^{-1})	Cooling rate/(°C·s^{-1})
TC1	777.1	85.0	14.5
TC2	1097.7	155.1	18.7
TC3	747.8	81.8	13.8
TC4	725.4	89.2	16.0

3.2 Mg−steel joint microstructures

MIG welding of AZ31B Mg alloy and Q235 low carbon steel was carried out at different welding parameters with AZ31 and AZ61 Mg alloy filler metals. The MIG welding parameters and heat inputs are listed in Table 5.

Table 5 MIG welding parameters and heat inputs used in this investigation

Experiment No.	Welding current/A	Arc voltage/V	Welding speed/(cm·min^{-1})	Heat input/(J·cm^{-1})
1	120	18	75	1210
2	125	20	75	1400
3	130	20	70	1562
4	130	20	65	1680
5	135	20	65	1744
6	135	22	65	1919
7	135	24	65	2093
8	140	24	65	2171
9	140	23	60	2254

The appearance of weld is one of important factors to evaluate welding quality. The experimental results indicate that welding heat input has a significant effect on the weld appearance, as shown in Fig. 4. At low welding heat input, the Mg alloy weld has small reinforcement due to less deposited metal (Fig. 4(a)), and the weld appearance is improved with an increase of the heat input (Fig. 4(b)), but excess heat input (2254 J/cm) increases the welding spatter and deteriorates the weld appearance, as shown in Fig. 4(c). It is necessary to select suitable welding heat input for improving the weld appearance quality. Based on above experimental results, the satisfactory weld appearance can be obtained in the welding heat inputs of 1744−2171 J/cm.

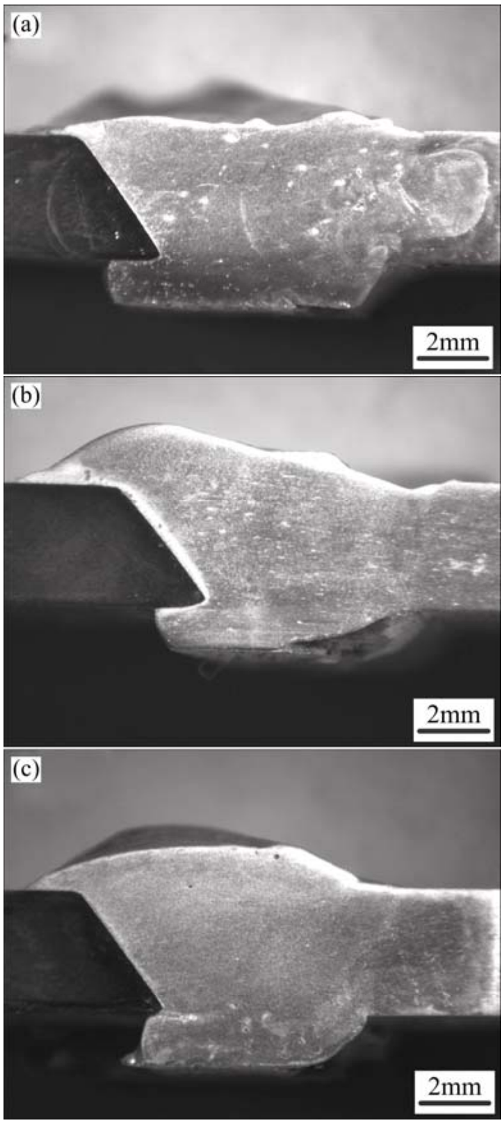

Fig. 4 Weld appearance with AZ31 filler metal at different heat inputs: (a) 1562 J/cm; (b) 2093 J/cm; (c) 2254 J/cm

Figure 5 illustrates typical microstructures of MIG welded Mg−steel joint. The joint includes weld zone, heat-affected zone in Mg alloy side (HAZ_1) and heat-affected zone in steel side (HAZ_2), as shown in Fig. 5(a). The chemical composition of welds depends on that of filler metals. With the AZ31 filler metal, Al content in the weld is 3.17%, and it increases to 6.20% when the AZ61 filler metal was used. From Figs. 5(b) and (c), it can be seen that both welds present the finer equiaxed grain structure (grain size of 10−13 μm),

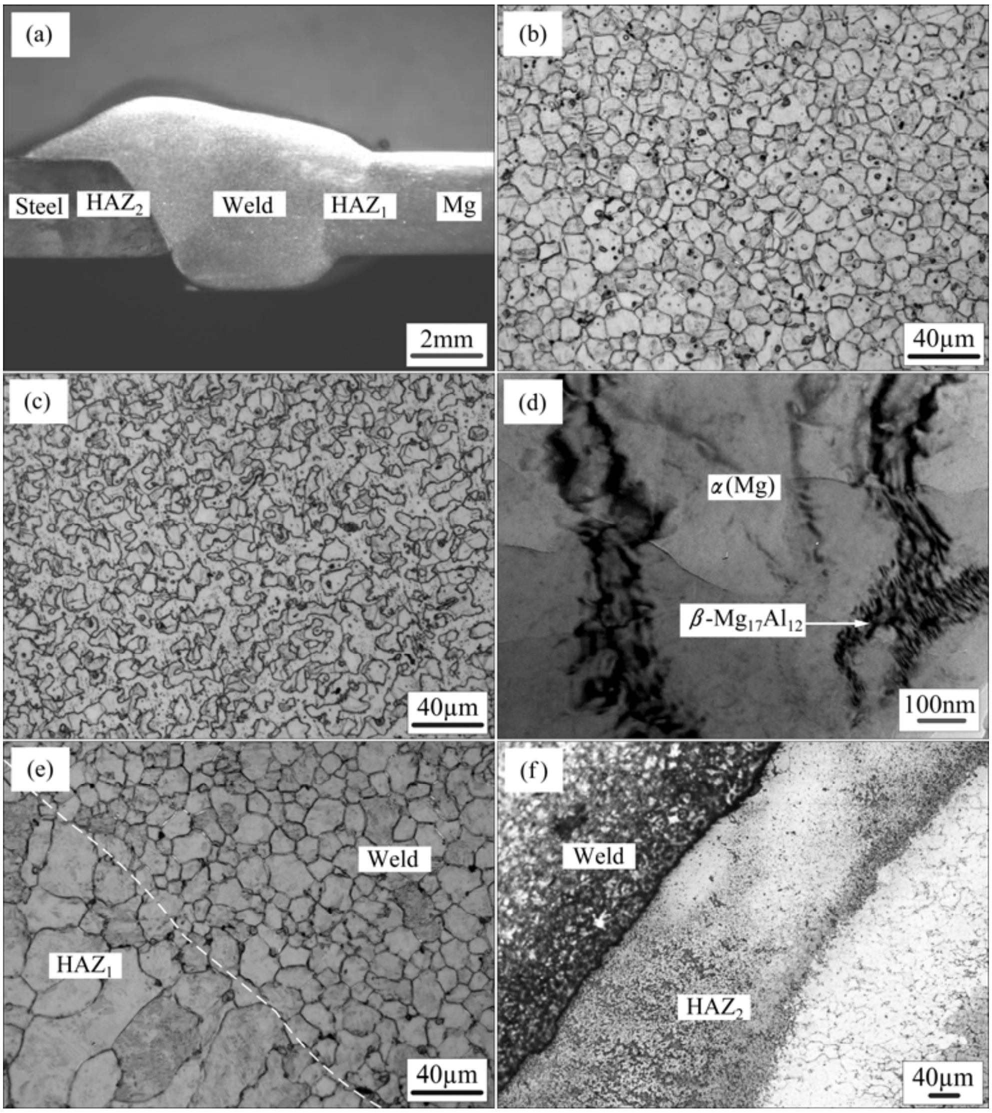

Fig. 5 Microstructures of Mg−steel joint: (a) Joint structure with AZ31 filler metal; (b) Weld with AZ31 filler metal; (c) Weld with AZ61 filler metal; (d) TEM image of weld with AZ61 filler metal; (e) HAZ_1 with AZ31 filler metal; (f) HAZ_2 with AZ31 filler metal

compared with Mg alloy base metal, due to very quick cooling rate for the welds. According to XRD analysis results (Fig. 6), the phase composition of the weld with 3.17% Al is mainly α(Mg) solid solution, similar to the Mg alloy base metal, while the α(Mg) and β-$Mg_{17}Al_{12}$ intermetallic compound were detected in the weld containing 6.20% Al, and the β-$Mg_{17}Al_{12}$ phases mainly distribute at α(Mg) grain boundaries (Fig. 5(d)). It is mainly associated with the increased weld Al content. From Fig. 5(e), it can also be seen that the Mg−steel joint has a typical fusion welding characteristic in the Mg alloy side, and the grain coarsens obviously in HAZ_1 due to welding heat effect. There exists a transition layer between Mg alloy weld and steel base metal, and HAZ_2 in steel side consists mainly of pearlite and ferrite, as shown in Fig. 5(f). During MIG welding, the Mg alloy was molten, whereas the steel retained solid. The joining of Mg and steel was achieved by means of the wetting and spreading of liquid Mg on solid steel surface and Mg/steel interface reaction to form the transition layer. Therefore, it has the characteristic of brazed joint in steel side.

In this investigation, the thickness of transition layers at Mg/steel interfaces depends on weld Al contents (Fig. 7). When weld Al content is 3.17%, the transition layer thickness is about 1.0 μm (Fig. 7(a)), and it increases to 2.5 μm (Fig. 7(b)) for the weld containing 6.20% Al. EDS analysis results indicate that the chemical composition of transition layers mainly includes Mg, Al and Fe elements. From Mg alloy weld to steel base metal across the transition layers, the concentration of Mg element decreases, that of Fe element increases, and the concentration of Al element has an increased tendency in the transition layers, as shown in Fig. 8. XRD was used to determine phase compositions of the transition layer. Since the fracture of Mg−steel joints occurred in the

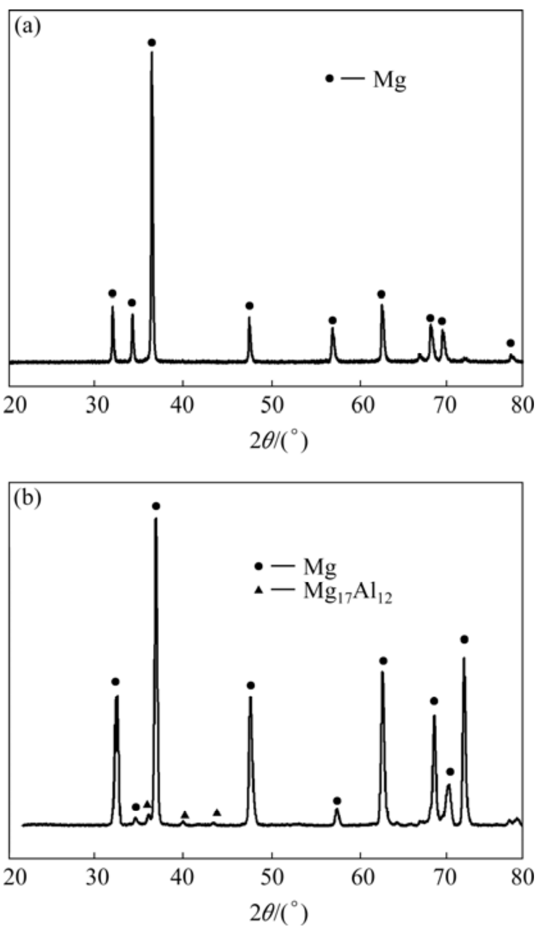

Fig. 6 XRD patterns of welds: (a) Weld with AZ31 filler metal; (b) Weld with AZ61 filler metal

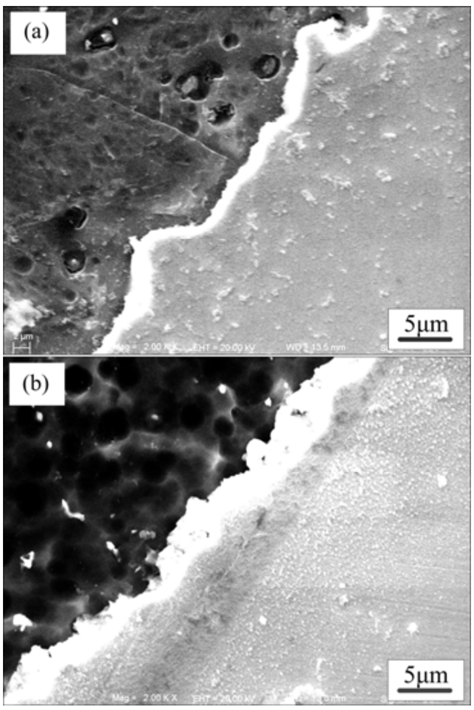

Fig. 7 Transition layers at Mg/steel interfaces: (a) Weld with 3.17% Al; (b) Weld with 6.20% Al

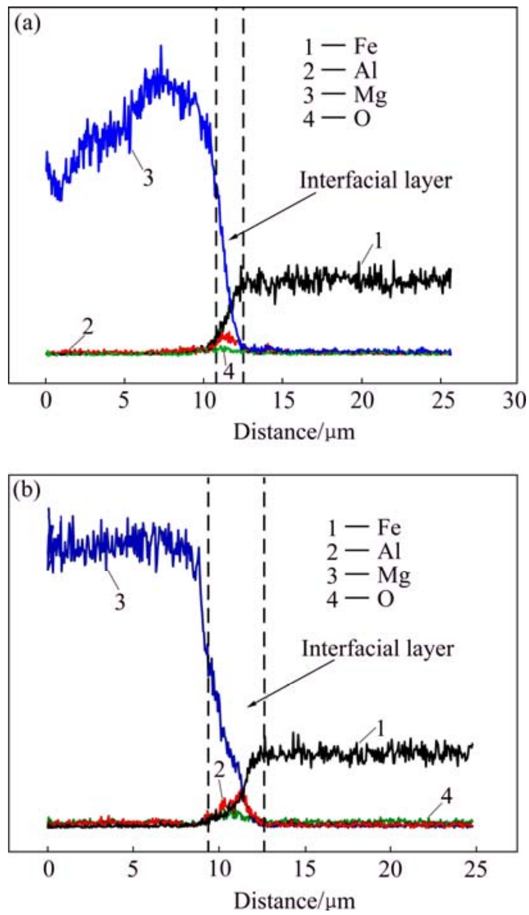

Fig. 8 Element distribution across transition layers: (a) Weld with 3.17% Al; (b) Weld with 6.20% Al

transition layer, XRD analysis was done on the joint fracture surface in steel side. The AlFe and $AlFe_3$ intermetallic compounds, and $Mg(Fe,Al)_2O_4$ metal oxide were detected in the transition layer (Fig. 9).

Based on above results, the inter-diffusion of Mg, Al and Fe elements occurred during MIG welding, and joining of Mg alloy and steel was realized by Mg/steel interface reaction. Since Mg and Fe do not react with each other to form binary compounds, Al plays an important role in the interface reaction. An increase of the transition layer thickness with increasing the weld Al content is mainly related to promoting Mg/steel interface reaction to form more Al−Fe compounds.

It should be pointed out that the temperature of Mg/steel interface also has an important effect on interface joining quality. Higher interface temperature favors the wetting and spreading of liquid Mg on solid steel surface, and promotes the element diffusion and interface reaction. The relative low interface temperature (747.8 °C) at the bottom of Mg/steel interface could result in discontinuous interface reaction layer (Fig. 10), affecting the interface joining quality.

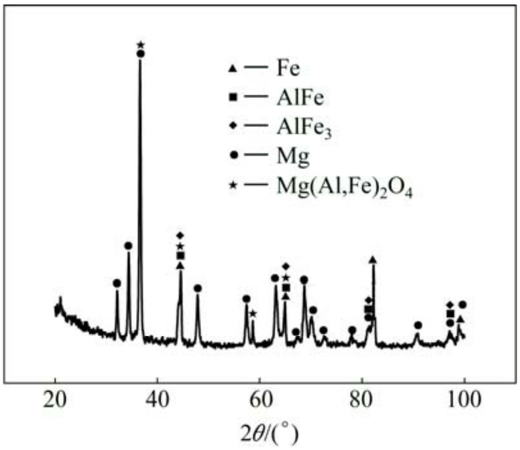

Fig. 9 XRD pattern of transition layer

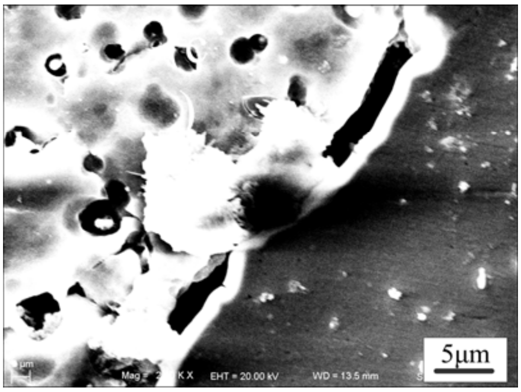

Fig. 10 Microstructures at bottom of Mg/steel interface

3.3 Mg−steel joint properties

The Vickers microhardness profiles across Mg−steel joints are illustrated in Fig. 11. From Fig. 11(a), it can be seen that the microhardness distribution is uneven. Mg alloy HAZ_1 has the lowest microhardness, which is mainly associated with the grain coarsening in this zone. Compared with HAZ_1, Mg alloy weld shows higher hardness values because it has a fine equiaxed grain structure. The highest hardness appears at the Mg/steel interface because it contains AlFe and $AlFe_3$ intermetallic compounds. The welding heat input has an effect on the joint microhardness (Fig. 11(b)). With an increase of the heat inputs, the microhardness decreases in HAZ_1 and increases at Mg/steel interface. It can be explained by forming coarser grain in HAZ_1 and more Al−Fe intermetallic compounds at Mg/steel interfaces.

The experimental results indicated that the welding heat input has a significant effect on the tensile strength of Mg−steel joints (Fig. 12). At low welding heat input the joint strength is very poor, it is improved obviously in the heat inputs of 1919−2254 J/cm, and the maximum joint strength (184.2 MPa) is achieved at the welding heat input of 2093 J/cm. The joint fracture mainly occurs at the Mg/steel interface layer (Fig. 13), indicating that

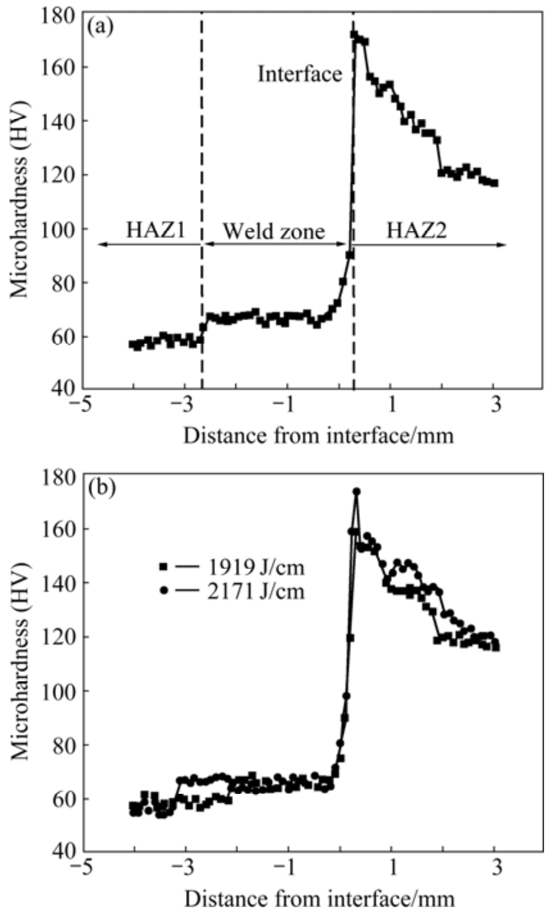

Fig. 11 Microhardness distributions of joints with AZ31 filler metal at different heat inputs: (a) 2093 J/cm; (b) 1919 J/cm and 2171 J/cm

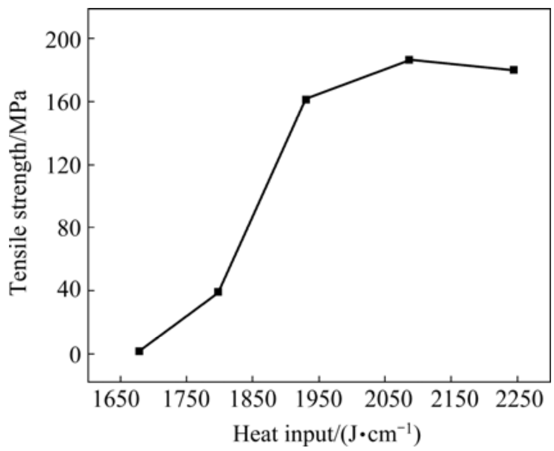

Fig. 12 Tensile strength of Mg−steel joints with AZ31 filler metal at different heat inputs

it is the weakest link in the Mg−steel joints.

In order to further clarify reasons for joint strength changes, the fracture surface morphology of Mg−steel joints was investigated. Figure 14 shows typical fracture surface morphologies in steel side. The fracture surface can be divided into two regions, Region A and Region B,

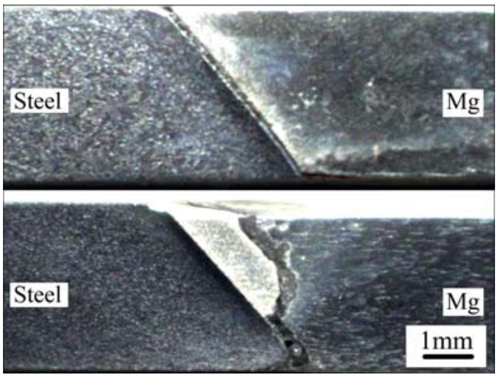

Fig.13 Fracture sites of Mg−steel joints with AZ31 filler metal

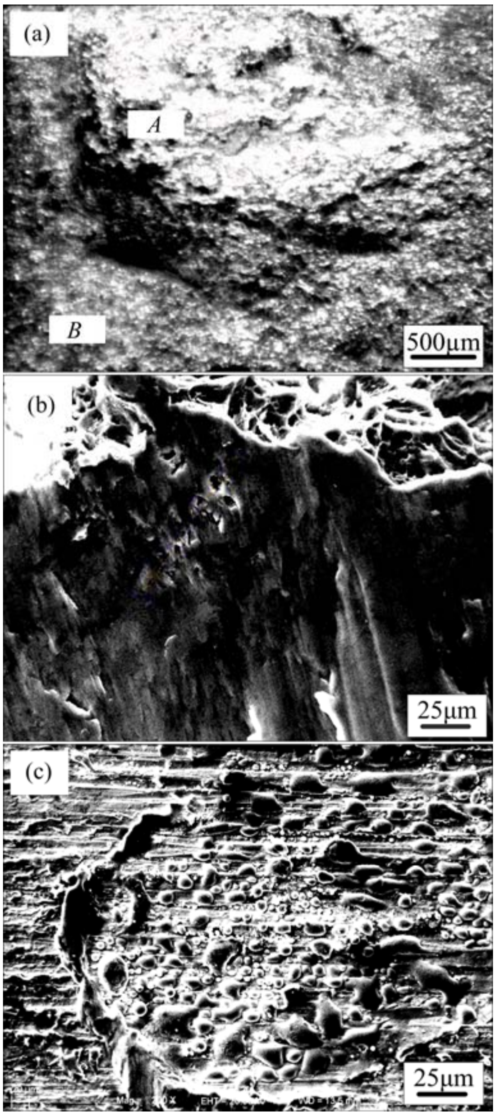

Fig. 14 Fracture surface morphologies of Mg−steel joint with AZ31 filler metal in steel side: (a) Macro-morphology; (b) Micro-morphology in Region *A*; (c) Micro-morphology in Region *B*

as shown in Fig. 14(a). In Region *A*, a large amount of retained Mg alloys are observed on the steel surface and there are some features of plastic deformation on the fracture surface (Fig. 14(b)), indicating that the sound joining is realized in this region. Hence, it is called the joined region in this investigation. The Region *B* is mainly located at the bottom of Mg/steel interface. Its fracture surface is relative smooth with less retained Mg alloy (Fig. 14(c)), which means that Mg alloy and steel are joined partially in this region. According to the weld thermal cycle curves at the Mg/steel interface, the bottom of the interface has the lowest peak temperature, which affects the element diffusion, interface reaction and joining quality. Figure 15 shows the ratio of areas between joined region and Mg/steel interface at different welding heat inputs. The higher the welding heat input, the larger the joined region area is, which is similar to the change of joint strength. Therefore, it is favorable to increase the welding heat input for improving the joining quality and joint strength.

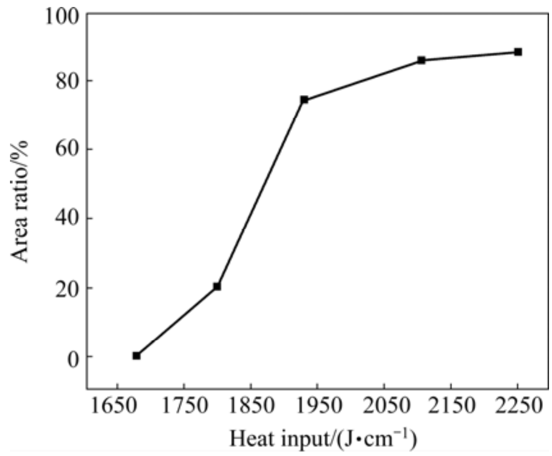

Fig. 15 Area ratio between joined region and interface at different heat inputs

In addition, in this investigation, it was found that Al content in the Mg alloy weld also has a significant effect on the tensile strength of Mg−steel joints. When the weld Al content is increased to 6.20%, the joint strength can reach 192 MPa. It is mainly related to the increased Al promoting Mg/steel interface reaction. Therefore, it is effective ways to select suitable welding heat input and weld Al content for improving the Mg−steel joint strength.

4 Conclusions

1) The joining of AZ31B Mg alloy to Q235 low carbon steel can be realized by the MIG welding process with Mg alloy filler metals. In the Mg−steel butt joint, there exist two kinds of joining mechanisms, the fusion welding in the Mg alloy side and brazing in steel side.

2) During MIG welding, the temperature distribution in the Mg−steel joint is uneven. The weld appearance and joint microstructures depend on the welding heat input and weld Al content. The satisfactory weld appearance is obtained in the heat inputs of 1744−2171 J/cm. Mg alloy welds containing 3.17% Al and 6.20% Al have fine equiaxed grain structure, consisting mainly of the α(Mg) and the α(Mg)+ β-$Mg_{17}Al_{12}$ phases, respectively. The transition layer at Mg/steel interface includes AlFe, $AlFe_3$ and $Mg(Fe,Al)_2O_4$ compounds. Increasing the weld Al content and heat input favors promoting the Mg/steel reaction to form the continuous interface transition layer.

3) The welding heat input and weld Al content have a significant effect on the Mg−steel joint strength. The joint strength increases obviously in the heat inputs of 1919−2254 J/cm. When the weld Al content is increased to 6.20%, the joint strength reaches 192 MPa, 80% of Mg alloy base metal strength. It is effective ways to select the suitable welding heat input and weld Al content for improving the Mg−steel joint strength.

References

[1] MASOUDIAN A, TAHAEI A, SHAKIBA A, SHARIFIANJAZI F, MOHANDESI J A. Microstructure and mechanical properties of friction stir weld of dissimilar AZ31-O magnesium alloy to 6061-T6 aluminum alloy [J]. Transactions of Nonferrous Metals Society of China, 2014, 24(5): 1317−1322.

[2] HAROONI M, CARLSON B, STROHMEIER B R, KOVACEVIC R. Pore formation mechanism and its mitigation in laser welding of AZ31B magnesium alloy in lap joint configuration [J]. Materials and Design, 2014, 58(6): 265−276.

[3] JIANG Ju-fu, WANG Ying, QU Jian-jun. Effect of process parameters on microstructure and properties of AM50A magnesium alloy parts formed by double control forming [J]. Transactions of Nonferrous Metals Society of China, 2014, 24(2): 321−333.

[4] LIU Xu-he, GU Shi-hai, WU Rui-zhi, LENG Xue-song, YAN Jiu-chun, ZHANG Mi-lin. Microstructure and mechanical properties of Mg−Li alloy after TIG welding [J]. Transactions of Nonferrous Metals Society of China, 2011, 21(3): 477−481.

[5] SUBRAVEL V, PADMANABAN G, BALASUBRAMANIAN V. Effect of welding speed on microstructural characteristics and tensile properties of GTA welded AZ31B magnesium alloy [J]. Transactions of Nonferrous Metals Society of China, 2014, 24(9): 2776−2784.

[6] WANG Yun-long, JIANG Zhao-hua, YAO Zhong-ping. Preparation and properties of ceramic coating on Q235 carbon steel by plasma electrolytic oxidation [J]. Current Applied Physics, 2009, 9: 1067−1071.

[7] MIAO Yu-gang, HAN Duan-feng, XU Xiang-fang, WU Bin-tao. Phase constitution in the interfacial region of laser penetration brazed magnesium–steel joints [J]. Materials Characterization, 2014, 93: 87−93.

[8] CHEN Y C, NAKATA K. Effect of tool geometry on microstructure and mechanical properties of friction stir lap welded Mg alloy and steel [J]. Materials and Design, 2009, 30: 3913−3919.

[9] WATANABE T, KAGIYA K, YANAGISAWA A. Solid state welding of steel and Mg alloy using a rotating pin [J]. Quarterly Journal of the Japan Welding Society, 2006, 24: 108−15.

[10] ELTHALABAWY W, KHAN T. Microstructural development of diffusion-brazed austenitic stainless steel to magnesium alloy using a nickel interlayer [J]. Materials Characterization, 2010, 61: 703−12.

[11] YAO Zhong-xiang, JIANG De-ping, PAN Chao, WANG Xiao-ming. Analysis about the jointing status for dissimilar metals of steel with magnesium [J]. Applied Mechanics and Materials, 2012, 233: 374−379.

[12] SCHNEIDER C, WEINBERGER T, INOUE J, KOSEKI T, ENZINGER N. Characterisation of interface of steel/Mg FSW [J]. Science and Technology of Welding & Joining, 2011, 16(1): 100−107.

[13] LIU L, XIAO L, FENG J, LI L, ESAEILI S, ZHOU Y. Bonding of immiscible Mg and Fe via a nanoscale Fe_2Al_5 transition layer [J]. Scripta Materialia, 2011, 65: 982−5.

[14] LIU L, XIAO L, FENG J C, TIAN Y H, ZHOU S Q, ZHOU Y. The mechanisms of resistance spot welding of magnesium to steel [J]. Metallurgical and Materials Transactions A—Physical Metallurgy and Materials Science, 2010, 41: 2651−61.

[15] QI Xiao-dong, SONG Gang. Interfacial structure of the joints between magnesium alloy and mild steel with nickel as interlayer by hybrid laser-TIG welding [J]. Materials and Design, 2010, 31: 605−609.

[16] LIU Li-ming, ZHAO Xu. Study on the weld joint of Mg alloy and steel by laser-GTA hybrid welding [J]. Materials Characterization, 2008, 59: 1279−1284.

[17] LIU Li-ming, QI Xiao-dong. Effects of copper addition on microstructure and strength of the hybrid laser-TIG welded joints between magnesium alloy and mild steel [J]. Journal of Materials Science, 2009, 44: 5725−5731.

[18] LIU Li-ming, QI Xiao-dong. Strengthening effect of nickel and copper interlayers on hybrid laser-TIG welded joints between magnesium alloy and mild steel [J]. Materials and Design, 2010, 31: 3960−3963.

[19] MIAO Yu-gang, HAN Duan-feng, YAO Jing-zheng, LI Feng. Effect of laser offsets on joint performance of laser penetration brazing for Mg alloy and steel [J]. Materials and Design, 2010, 31: 3121−3126.

[20] MIAO Yu-gang, HAN Duan-feng, YAO Jing-zheng, LI Feng. Microstructure and interface characteristics of laser penetration brazed Mg alloy and steel [J]. Science and Technology of Welding & Joining, 2010, 15: 97−103.

[21] DONG Hong-guang, LIAO Chuan-qing, YANG Li-qun. Microstructure and mechanical properties of AZ31B magnesium alloy gas metal arc weld [J]. Transactions of Nonferrous Metals Society of China, 2012, 22(6): 1336−1341.

[22] TAY K M, BUTLER C. Modelling and optimizing of a MIG welding process—A case study using experimental designs and neural networks [J]. Quality and Reliability Engineering International, 1997, 13: 61−70.

[23] EASTERLING K. Introduction to the physical metallurgy of welding (second edition) [M]. 2nd ed. Great Britain: Butterworth-Heinemann, 1992: 27−33.

镁−钢异种金属 MIG 焊接头的显微组织与力学性能

汪晓勇，孙大千，殷世强，刘东阳

吉林大学 材料科学与工程学院，汽车材料教育部重点实验室，长春 130025

摘　要：采用熔化极惰性气体保护电弧焊方法(MIG)实现镁合金和低碳钢的连接，并研究焊接热循环特点和镁−钢对接接头的显微组织及力学性能。研究结果表明，在焊接过程中，接头的温度场分布是不均匀的。镁合金焊缝金属为细小的等轴晶结构。在镁/钢界面存在主要由 AlFe、$AlFe_3$ 和 $Mg(Fe,Al)_2O_4$ 相组成的过渡层，这一过渡层是镁−钢接头的最薄弱环节。焊接线能量和焊缝 Al 含量对镁−钢接头的抗拉强度具有明显的影响。焊接线能量由 1680 J/cm 增至 2093 J/cm，接头强度明显增加，这主要归因于镁/钢界面反应。增加焊缝 Al 含量至 6.20%，镁−钢接头强度可达 192 MPa，为 AZ31 镁合金母材强度的 80%。因此，选择合适的焊接线能量和焊缝 Al 含量有利于改善镁−钢接头的抗拉强度。

关键词：AZ31B 镁合金；Q235 钢；熔化极惰性气体保护电弧焊；异种金属连接

(Edited by Yun-bin HE)